Frequency-independent radiation modes of interior sound radiation: An analytical study

C. Hesse[a,*], J. M. Vivar Perez[a], M. Sinapius[b]

[a] *Institute of Composite Structures and Adaptive Systems, German Aerospace Center (DLR), Sportallee 54a, 22335 Hamburg, Germany*
[b] *Institute of Adaptronic and Functional Integration, Langer Kamp 6, 38106 Braunschweig, Germany*

Abstract

Global active control methods of sound radiation into acoustic cavities necessitate the formulation of the interior sound field in terms of the surrounding structural velocity. This paper proposes an efficient approach to do this by presenting an analytical method to describe the radiation modes of interior sound radiation. The method requires no knowledge of the structural modal properties, which are often difficult to obtain in control applications. The procedure is exemplified for two generic systems of fluid-structure interaction, namely a rectangular plate coupled to a cuboid cavity and a hollow cylinder with the fluid in its enclosed cavity. The radiation modes are described as a subset of the acoustic eigenvectors on the structural-acoustic interface. For the two studied systems, they are therefore independent of frequency.

Keywords: active control, ASAC, radiation modes, fluid-structure interaction

1. Introduction

The active control of structural sound radiation is divided into the categories active vibration control [1] (AVC), active noise and vibration control [2] (ANVC) and active structural-acoustic control [3] (ASAC). ANC and ANVC deal with the active reduction of structural vibration levels or acoustic pressure levels respectively. This is achieved by using structural actuators. For ASAC applications, comprehensive literature exists describing the sound radiation into the acoustic far field [4, 5]. In problems of noise reduction in enclosed spaces or cavities, the quantity to be controlled is commonly based on the volume-averaged acoustic pressure levels, i. e. the acoustic potential energy (APE) [6]. In the last case it is usual to express the APE as a linear combination of contributions from each interior radiation mode. The interior radiation modes are orthogonal functions that describe vibration modes of the structure, such that

*Corresponding author
Email address: christian.hesse@dlr.de (C. Hesse)

the contribution from each one of them to the APE in the enclosed fluid is uncoupled from any other. In recent studies [7, 8, 9, 10] this formulation is based on the orthonormal decomposition of the error weighting matrix. The error weighting matrix relates the velocity of a vibrating structure to the acoustic potential energy in an adjacent fluid-filled cavity and is usually assembled using the modal interaction theory. If a weak coupling between the structure and the cavity fluid is assumed, the calculation of vibration modes can be performed separately for the structure and the fluid respectively [11]. Using this method, disregard of high-frequency vibration modes can lead to an inaccurate calculation of the error weighting matrix and the radiation modes likewise.

Snyder and Tanaka describe the interior radiation modes and efficiencies based on an analytical study of a plate coupled to a rectangular enclosure in [7]. The radiation modes are based on a frequency dependent orthonormal decomposition of the error weighting matrix. The modal interaction approach is employed, using 30 acoustic and structural modes. The interior radiation modes, calculated from the orthonormal matrix decomposition are shown to resemble the cavity modes at the interaction plane. An independence from frequency is not mentioned.

The implementation of active control of sound radiation in an irregular shaped cavity is investigated by Cazzolato et al. [8], using structural error sensors. The acoustic potential energy is related via the error weighting matrix to the structural modes based on a discrete set of structural measurements. The error weighting matrix is assembled by utilizing the modal interaction theory, coupling numerically calculated cavity and structural vibration modes. Decomposing the error weighting matrix, the orthogonal modes of sound radiation into the cavity are calculated. The interior radiation modes presented by Cazzolato [8] depend on frequency.

Cazzolato et al. [12] propose the definition of the interior radiation modes as the cavity modes at the interaction plane. The cavity modes, however, are not a set of orthogonal eigenvectors at the interaction plane, as described by Johnson in [9]. Therefore the error weighting matrix is not diagonalized by the cavity modes, which is a requirement for using the interior radiation modes for real-time active control applications.

The interior radiation modes are used by Johnson [9, 10], here termed principle velocity patterns, to tailor the structural-acoustic-coupling for an optimal sound radiation into a cylindrical cavity. The calculation of these velocity patterns is based on a frequency-dependent singular value decomposition of the error weighting matrix. Since the singular value decomposition is performed at every frequency step, the singular values are sorted based on the orthogonality properties of the singular vectors. Although a similarity in the numerical results of the singular vectors for different frequencies is observed, an independence of frequency is not conclusively proven.

The concept of interior radiation modes is also used by Bagha et al. in [13] for structural sensing of the acoustic potential energy. In order to reduce the number of sensors necessary, a numerical study is conducted, using the modal interaction approach. For a rectangular plate, coupled to a cuboid cavity, a

frequency-dependence of the interior radiation modes is described. This dependence is illustrated by a reference to the exterior radiation modes [4]. The exterior radiation modes are derived from the radiation resistance matrix, which is assembled using the elemental radiator approach [11]. These exterior radiation modes do not include any coupling selectivity to acoustic eigenvectors. The dependence of the radiation resistance between elemental radiators on frequency is responsible for the exterior radiation modes frequency-dependence.

In summary, it can be seen, that most of this research regarding the interior radiation modes is done using an orthonormal decomposition of the error weighting matrix. When using the modal coupling theory for the purpose of assembling the error weighting matrix, numerous eigenvectors of the uncoupled systems are required to correctly describe the physical coupling. The quality of the modal solution as well as the level of the numerical discretisation are expected to be correlated to the frequency dependence of the interior radiation modes. To the authors' knowledge the interior radiation modes have not yet been calculated using an analytic formulation, which is the aim of this study. This formulation utilizes specific properties of the cavity mode shapes at the interaction plane. This allows assembling the interior radiation modes as a subset of the cavity modes at the interaction plane, which makes them in return independent from frequency. The objective of this paper is to calculate these radiation modes, which only show self-radiation efficiency, for generic coupled systems and verify their frequency-independence. It is the aim, to make the radiation modes utilizable for real-time applications of active reduction approaches, designed to minimize the global sound radiation into cavities.
The foundation for the analytical radiation mode evaluation is given in section 2, where the APE is described in terms of the surrounding structural velocity. Section 3 expands the general formulation for two specific coupled fluid-structure systems and examines the interior radiation modes. The first model is a rectangular plate coupled to a cuboid fluid cavity. The other one is a cylindrical shell coupled to an interior cavity. It is shown, for the two models considered, that the interior radiation modes are independent of frequency, as they belong to a subset of the cavity modes orthogonal at the interaction plane. The frequency-independent radiation modes and efficiencies are presented in section 4. Finally, in section 5 the paper is concluded and an outlook to future research activities is given.

2. Acoustic potential energy evaluation

This section presents the theoretical foundation for the evaluation of the interior radiation modes. It will result in a formulation of the APE in dependence of the surrounding structural velocity.
A graphical representation of the noise radiation into a cavity along with the boundary conditions considered is shown in Figure 1. A vibrating structural surface S is coupled to an interior volume V filled with a fluid, e.g. air. The vector $\mathbf{n}$ describes the unit normal vector on the structural surface. The interior

fluid reacts as a forced vibration to the structural excitation and can also lead to an excitation of the structure. The surface S_r represents an acoustically rigid boundary condition.
The time-averaged APE $E(\omega)$ inside the volume V is proportional to the volume average of the mean squared acoustic pressure p [6]

$$E(\omega) = \frac{1}{4\rho c^2} \int_V |p(\mathbf{r}, \omega)|^2 dV, \tag{1}$$

where ρ and c are the fluid density and acoustic velocity respectively. Here, ω is the angular frequency. The coordinate vector $\mathbf{r}$ describes points in the acoustic domain V.

The acoustic pressure can be expressed as a linear combination of cavity modes

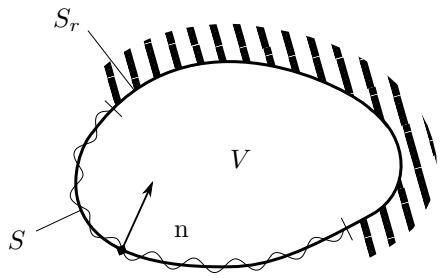

Figure 1: Graphical representation of noise radiation from a vibrating structural surface S into a cavity volume V with acoustically rigid boundary conditions at S_r

(orthogonal mode shape functions) $\Phi_j(\mathbf{r})$ as

$$p(\mathbf{r}, \omega) = \sum_{j=1}^{\infty} q_j(\omega) \Phi_j(\mathbf{r}) \tag{2}$$

with $q_j(\omega)$ being the amplitude of the j-th cavity mode. With equation (2), the APE is rewritten as

$$E(\omega) = \frac{1}{4\rho c^2} \sum_{j=1}^{\infty} \Gamma_j |q_j(\omega)|^2, \tag{3}$$

with the volume normalization factor

$$\Gamma_j = \int_V |\Phi_j(\mathbf{r})|^2 \, dV. \tag{4}$$

The aim of this section is to express the APE in terms of the surrounding structural velocity $v(\mathbf{r}_s, \omega)$ of the points at the surface S. For that reason, the transfer function from the structural velocity to the acoustic pressure $p(\mathbf{r}, \omega)$

from the Kirchhoff-Helmholtz integral equation is considered [6], which simplifies to

$$p(\mathbf{r},\omega) = i\rho\omega \int_S v(\mathbf{r}_s,\omega)\mathcal{G}(\mathbf{r}|\mathbf{r}_s,\omega)dS, \tag{5}$$

when there are no sources inside the cavity. In equation (5), $\mathbf{r}_s$ is the position vector of the points in the structural domain S and $i = \sqrt{-1}$ the complex unit. The function $v(\mathbf{r}_s,\omega)$ is the normal velocity on the structural boundary S in contact with the fluid and $\mathcal{G}(\mathbf{r}|\mathbf{r}_s,\omega)$ is the Green's function [6] satisfying rigid walled boundary conditions

$$\mathcal{G}(\mathbf{r}|\mathbf{r}_s,\omega) = \sum_{j=1}^{\infty} \frac{\Phi_j(\mathbf{r})\Phi_j(\mathbf{r}_s)}{\Gamma_j(\kappa_j^2 + 2i\zeta_j\kappa_j k - k^2)}. \tag{6}$$

In equation (6), k describes the frequency-dependent wave number $k = \frac{\omega}{c}$ and κ_j the resonant wave number of the j-th cavity mode. The modal damping ratio of the j-th cavity mode is denoted by ζ_j. Substituting equations (2) and (6) into equation (5) yields an expression for the j-th frequency dependent modal amplitude

$$q_j(\omega) = \frac{i\omega\rho}{\Gamma_j(\kappa_j^2 + 2i\zeta_j\kappa_j k - k^2)} \int_S \Phi_j(\mathbf{r}_s)v(\mathbf{r}_s,\omega)dS. \tag{7}$$

This expression is introduced in equation (3) to obtain

$$E(\omega) = \sum_{j=1}^{\infty} s_j(\omega) \left| \int_S \Phi_j(\mathbf{r}_s)v(\mathbf{r}_s,\omega)dS \right|^2. \tag{8}$$

In equation (8), the radiation efficiency $s_j(\omega)$ of the j-th cavity mode is

$$s_j(\omega) = \frac{\rho c^2}{4\Gamma_j} \left| \frac{i\omega}{(\omega_j^2 + 2i\zeta_j\omega_j\omega - \omega^2)} \right|^2. \tag{9}$$

Equation (8) describes the APE in the acoustic domain V depending on the contribution of the structural velocity $v(\mathbf{r}_s,\omega)$ to the cavity modes $\Phi_j(\mathbf{r}_s)$ on the vibrating surface S. The cavity modes $\Phi_j(\mathbf{r}_s)$ are orthogonal along the fluid domain V and therefore do not describe independent contributions of the structural vibration to the APE. The next section will show, that it is possible to obtain an orthogonal formulation of the cavity modes on the structural surface S for the exemplary systems.

3. Analytical Study

This section applies the aforementioned formulation for the APE to two particular models of structural-acoustic interaction systems, which vibration and cavity modes are well known [14] and can be analytically described. The properties of the cavity mode shapes at the interaction plane are investigated and the resulting interior radiation modes calculated.

3.1. Rectangular plate-cavity system

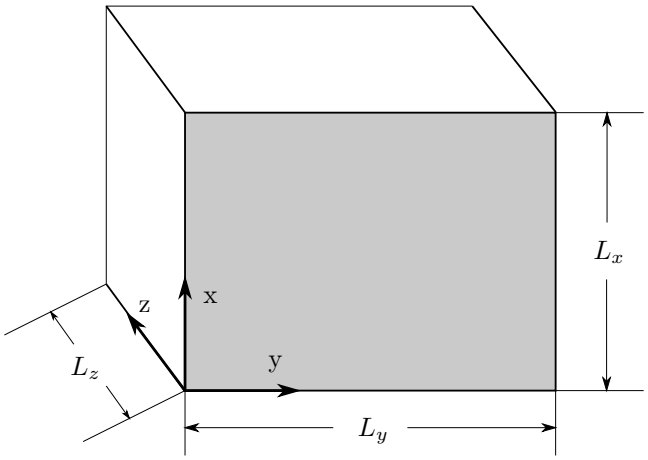

Figure 2: Rectangular plate (gray) with cuboid cavity

The first model to be analysed is a rectangular thin plate coupled to a cuboid cavity. The model is shown in Figure 2. The acoustic cavity is surrounded by five acoustically rigid walls and one structural, elastic wall at $z = 0$.
The mode shapes for the acoustic domain with dimensions $(L_x \times L_y \times L_z)$ as well as rigid cavity walls are written as

$$\Phi_{l,m,n}(x, y, z) = \cos\left(\frac{l\pi x}{L_x}\right) \cos\left(\frac{m\pi y}{L_y}\right) \cos\left(\frac{n\pi z}{L_z}\right), \tag{10}$$

with the modal indices $l, m, n \in \mathbb{N}_0$ [14]. Here, $\mathbb{N}_0$ describes the non-negative natural numbers. According to [15, 16] it is appropriate to use the rigid walled cavity modes, since their mode shapes will not change significantly in the coupled system when the structure is not thin and the acoustic medium is not dense. The validity of such an approach as well as its limitations are investigated in [17]. From this it can be concluded, that using the uncoupled cavity mode approach the interior pressure distribution can be accurately modelled.
The acoustic eigenfrequencies [14] are calculated as

$$\omega_{l,m,n} = c\pi \sqrt{\left(\frac{l}{L_x}\right)^2 + \left(\frac{m}{L_y}\right)^2 + \left(\frac{n}{L_z}\right)^2}. \tag{11}$$

Evaluating equation (4) for the acoustic mode shapes in equation (10) yields the volume normalization factors for the cuboid cavity

$$\Gamma_{l,m,n} = \frac{L_x L_y L_z}{8} \epsilon_l \epsilon_m \epsilon_n \tag{12}$$

with

$$\epsilon_l = \begin{cases} 2 & , l = 0 \\ 1 & , \text{otherwise.} \end{cases} \tag{13}$$

We can see from equation (10), that the cavity mode shape $\Phi_{l,m,n}(x,y)\Big|_{z=0}$ constrained to the interaction plane $z = 0$ does not depend on the modal index n. To examine the properties of the cavity modes at the interaction plane, the inner product on L^2 is considered

$$\langle f, g\rangle = \int_S f(\mathbf{r}_s) g^*(\mathbf{r}_s) dS \tag{14}$$

for the two arbitrary functions $f(\mathbf{r}_s)$ and $g(\mathbf{r}_s)$, where * describes the complex conjugate. The cavity modes constrained to the interaction plane are rewritten as $u_{l,m}(x,y) = \Phi_{l,m,n}\Big|_{z=0}$. Evaluating the inner product from equation (14) for $u_{l,m}(x,y)$ yields

$$\left| \frac{\langle u_{l_1,m_1}, u_{l_2,m_2}\rangle}{\sqrt{\langle u_{l_1,m_1}, u_{l_1,m_1}\rangle}\sqrt{\langle u_{l_2,m_2}, u_{l_2,m_2}\rangle}} \right| = \begin{cases} 1 & \text{, if } l_1 = l_2 \text{ and } m_1 = m_2 \\ 0 & \text{, otherwise.} \end{cases} \tag{15}$$

They are orthogonal along the structural surface S. It should be mentioned, that radiation modes are defined to only show self-radiation efficiencies and no mutual radiation efficiencies. According to equation (15), the structural radiation modes $u_{l,m}(x,y)$ fulfil this condition and can therefore be derived from the cavity modes with indices (l,m) as

$$u_{l,m}(x,y) = \cos\left(\frac{l\pi x}{L_x}\right)\cos\left(\frac{m\pi y}{L_y}\right). \tag{16}$$

Note that these radiation modes are independent of frequency. The radiation efficiency of each radiation mode $u_{l,m}(x,y)$ is then a sum of contributions from each cavity mode $\Phi_{l,m,n}$ with $n = 0, 1, 2, \ldots$. Since cavity modes with different modal indices n contribute to one radiation mode, the radiation efficiencies from equation (9) can be restated as

$$s_{l,m}(\omega) = \sum_{n=0}^{\infty} \frac{\rho c^2}{4\Gamma_{l,m,n}} \left| \frac{i\omega}{\omega_{l,m,n}^2 + 2i\zeta_{l,m,n}\omega_{l,m,n}\omega - \omega^2} \right|^2. \tag{17}$$

The APE inside the cuboid cavity can than be rewritten as

$$E(\omega) = \sum_{l,m=0}^{\infty} s_{l,m}(\omega) \left|\langle u_{l,m}, v(\omega)\rangle\right|^2. \tag{18}$$

The cavity modes have been shown analytically to be either orthogonal or parallel along the interaction surface in this section. The structural radiation modes $u_{l,m}(x,y)$ for the rectangular plate are therefore independent of frequency. The next section evaluates these properties for a second model.

3.2. Cylindrical plate-cavity system

The second model of the cylindrical plate-cavity system is depicted in figure 3 in the cylindrical coordinate system (r, θ, z). The circumferential structural surface at $r = R$ represents an elastic boundary for the fluid, while the cylinder caps at $z = 0$ and $z = L_z$ are rigid. For the cylindrical fluid-structural interaction,

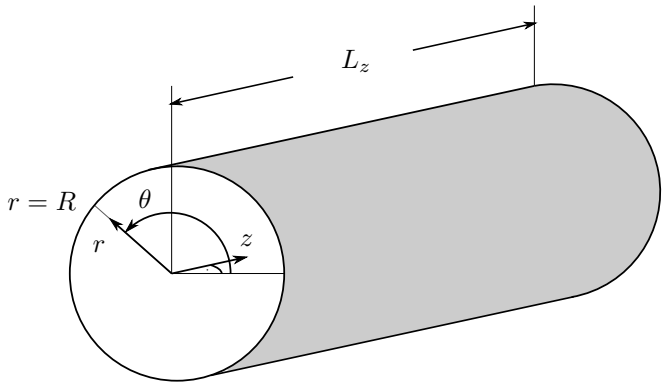

Figure 3: Cylindrical shell (gray) with interior cavity

the uncoupled cavity mode shapes [14] can be written as

$$\Phi_{l,m,n}(r, \theta, z) = \cos\left(\frac{l\pi z}{L_z}\right) J_m(\gamma_{m,n}\frac{r}{R}) \left(\sin(m\theta) + \cos(m\theta)\right), \tag{19}$$

where J_m describes the m-th bessel function of the first kind. Here, $l, m, n \in \mathbb{N}_0$ describe the axial, circumferential and radial modal indices respectively. In equation (19), the scalar $\gamma_{m,n}$ is the n-th zero of the derivative of the m-th bessel function, so that $J'_m(\gamma_{m,n}) = 0$. The acoustic eigenfrequencies [14] are

$$\omega_{l,m,n} = c\sqrt{\gamma^2_{m,n} + \left(\frac{l\pi}{L_z}\right)^2} \tag{20}$$

Evaluating equation (4) for the cavity mode shapes in equation (19) yields the volume normalization factors for the cylindrical enclosure

$$\Gamma_{l,m,n} = \left(1 - \frac{m^2}{\gamma^2_{m,n}}\right) \frac{J^2_m(\gamma_{m,n})}{2} \pi R^2 L_z \epsilon_l \tag{21}$$

with

$$\epsilon_l = \begin{cases} 2 & , l = 0 \\ 1 & , l \neq 0. \end{cases} \tag{22}$$

It can be seen from equation (19), that each of the cavity modes $\Phi_{l,m,n}\Big|_{r=R}$ with given indices (l, m) differs from each other depending on the radial modal

index n. This is different to the cuboid cavity system, where an independence of the modal index n in z-direction is observed. This means, that the cavity modes with different radial modal indices n can be multiples of one another. The cavity modes on the interaction plane ($r = R$) are rewritten as $u_{l,m}(\theta, z) = \Phi_{l,m,n=0}\Big|_{r=R}$. The inner product according to equation (14) is evaluated for $u_{l,m}(\theta, z)$, which yields

$$\begin{aligned}\left|\frac{\langle u_{l_1,m_1,n_1}, u_{l_2,m_2,n_2}\rangle}{\sqrt{\langle u_{l_1,m_1,n_1}, u_{l_1,m_1,n_1}\rangle}\sqrt{\langle u_{l_2,m_2,n_2}, u_{l_2,m_2,n_2}\rangle}}\right| \\ = \begin{cases} 1 & \text{, if } l_1 = l_2 \text{ and } m_1 = m_2 \\ 0 & \text{, otherwise.} \end{cases}\end{aligned} \tag{23}$$

The structural radiation modes $u_{l,m}(\theta, z)$ are orthogonal along the structural interface S. The radiation modes $u_{l,m}(\theta, z)$ as well as the radiation efficiencies $s_{l,m}(\omega)$ are therefore rewritten as

$$u_{l,m}(\theta, z) = \cos\left(\frac{l\pi z}{L_z}\right)\left(\sin(m\theta) + \cos(m\theta)\right), \tag{24}$$

and

$$s_{l,m}(\omega) = \sum_{n=0}^{\infty} \frac{\rho c^2}{4\Gamma_{l,m,n}} \left|\frac{i\omega\alpha_{m,n}}{\omega_{l,m,n}^2 + 2i\zeta_{l,m,n}\omega_{l,m,n}\omega - \omega^2}\right|^2. \tag{25}$$

respectively. The factor $\alpha_{m,n}$ from equation (25) is substituted as the ratio of the cavity modes with different axial modal indices n

$$\alpha_{m,n} = \frac{J_m(\gamma_{m,n})}{J_m(\gamma_{m,n=0})}. \tag{26}$$

In accordance to the rectangular plate, the interior radiation modes for the cylindrical plate are independent of frequency. The APE can again be rewritten as

$$E(\omega) = \sum_{l,m=0}^{\infty} s_{l,m}(\omega)\left|\langle u_{l,m}, v(\omega)\rangle\right|^2 \tag{27}$$

for the cylindrical enclosure.

4. Frequency-independent interior radiation modes

This section presents the above calculated radiation efficiencies as well as the frequency-independent radiation modes for the two fluid-structure-interaction systems. For the following calculations, an acoustic fluid density of 1.204 $\frac{\text{kg}}{\text{m}^3}$ and a speed of sound of 343 $\frac{\text{m}}{\text{s}}$ is assumed. An acoustic modal damping ratio for all modes of $\zeta_{l,m,n} = 0.01$ is considered.

4.1. Radiation modes of the rectangular plate-cavity system

The radiation modes for the rectangular plate-cavity system according to section 3.1 are evaluated and presented in this section. The structural plate has dimensions of $(L_x \times L_y) = (0.8 \times 0.6)$ m^2, while the cavity has a depth of $L_z = 0.42$ m. Five resulting radiation efficiencies from equation (17) for the interior sound radiation into the cuboid cavity are shown in Figure 4. They exhibit several resonance peaks, which occur at the acoustic eigenfrequencies which are associated with the radiation modes. The acoustic eigenfrequencies, calculated from equation (11) are shown in table 1.

The eigenfrequencies of the cavity modes coincide with the peaks in radiation

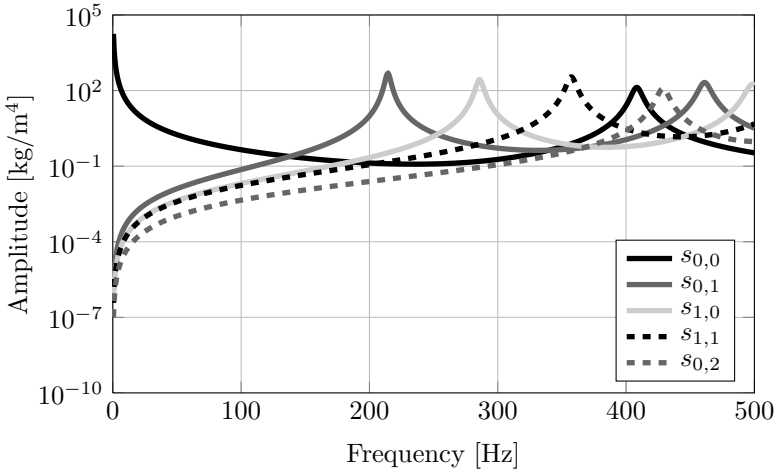

Figure 4: Radiation efficiencies for the interior radiation into the cuboid cavity

Table 1: Acoustic eigenfrequencies of cuboid cavity

(l, m, n)	eigenfrequency $\omega_{l,m,n}/(2\pi)$
$(0, 0, 0)$	0 Hz
$(0, 1, 0)$	214.37 Hz
$(1, 0, 0)$	285.83 Hz
$(1, 1, 0)$	357.29 Hz
$(0, 0, 1)$	408.33 Hz
$(0, 2, 0)$	428.75 Hz
$(0, 1, 1)$	461.18 Hz
$(1, 0, 1)$	498.43 Hz

efficiency of the respective radiation mode. Additional peaks occur in each radiation efficiency due to the cavity modes with identical mode shapes on the interaction plane. In accordance with the analytical expression given in equation 17, the two peaks in radiation efficiency 1 at 0 Hz and $\approx$ 408 Hz belong

to the cavity modes $(l, m, n) = (0, 0, 0)$ and $(l, m, n) = (0, 0, 1)$. In other words, every combination of (l, m) yields one radiation mode independent from n. Each efficiency of these radiation modes peaks at the acoustic eigenfrequencies of the associated index n.

Five radiation modes are shown in Figure 5. These correspond to the cavity modes on the interaction plane. Additional modes with a modal index $n > 0$ can therefore be neglected for the evaluation of the interior sound field.

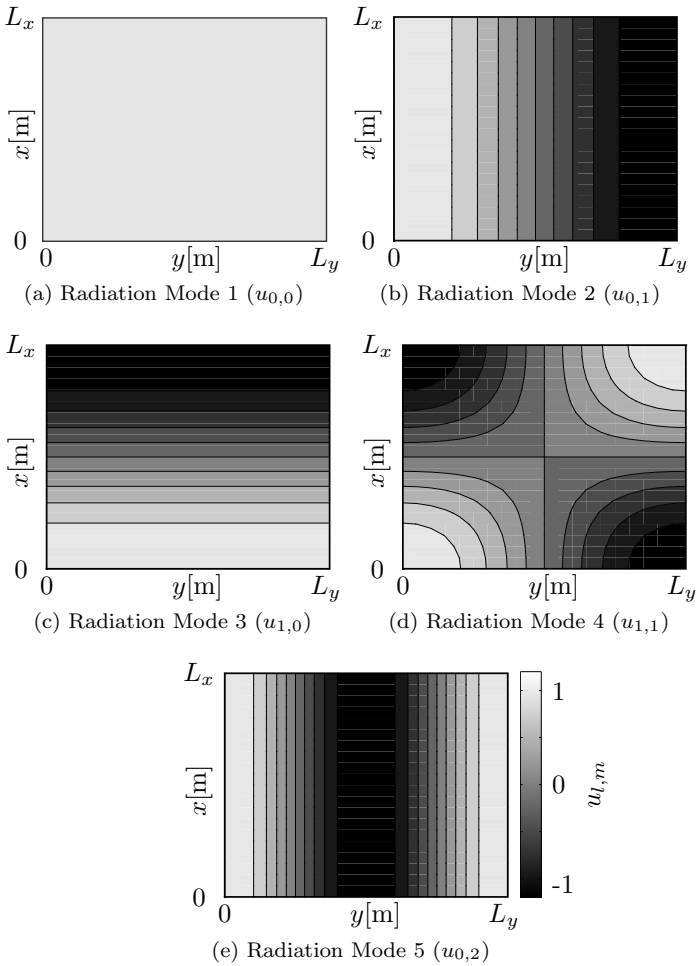

(a) Radiation Mode 1 ($u_{0,0}$)
(b) Radiation Mode 2 ($u_{0,1}$)
(c) Radiation Mode 3 ($u_{1,0}$)
(d) Radiation Mode 4 ($u_{1,1}$)
(e) Radiation Mode 5 ($u_{0,2}$)

Figure 5: Radiation modes for the interior radiation into the cuboid cavity

4.2. Radiation modes of the cylindrical plate-cavity system

The dimensions of the cylindrical plate-cavity system in accordance with section 3.2 are $(R \times L_z) = (0.5 \times 3)$ m^2. The radiation efficiencies 1-6 and 7-12

of the radiation into the cylindrical cavity are shown in figure 6 and figure 7 respectively. This numbering results from sorting according to an ascending eigenfrequency of the fundamental cavity mode. In comparison to the cuboid cavity, a higher density of cavity modes in the considered frequency regime can be observed. This is due to the bigger volume of the cylindrical cavity. Several resonances per radiation mode occur at multiples of the radial modal index n. The corresponding eigenfrequencies of the radiation modes 1-6, calculated from equation (20) are listed in table 2. The radiation modes 1-6 of the cylindrical

Table 2: Acoustic eigenfrequencies of cylindrical cavity

(l,m,n)	eigenfrequency $\omega_{l,m,n}/(2\pi)$	(l,m,n)	eigenfrequency $\omega_{l,m,n}/(2\pi)$
$(0,0,0)$	0 Hz	$(0,0,1)$	418.32 Hz
$(1,0,0)$	57.17 Hz	$(1,0,1)$	422.21 Hz
$(2,0,0)$	114.34 Hz	$(2,0,1)$	433.67 Hz
$(3,0,0)$	171.50 Hz	$(3,0,1)$	452.11 Hz
$(0,1,0)$	201.00 Hz	$(0,1,1)$	582.09 Hz
$(1,1,0)$	208.97 Hz	$(1,1,1)$	584.89 Hz

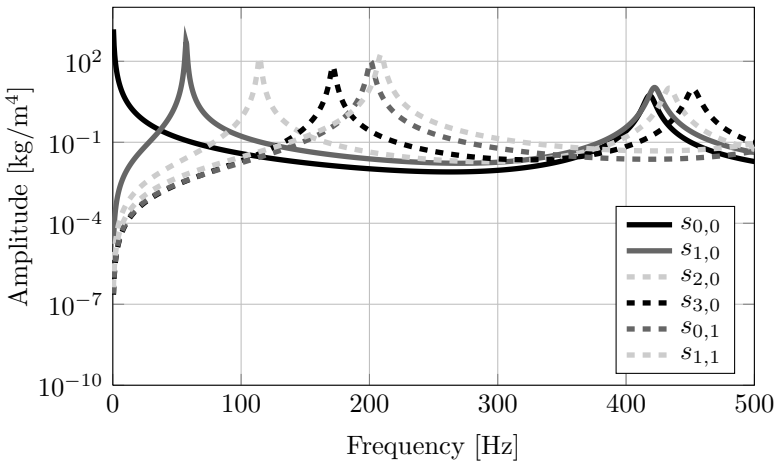

Figure 6: Radiation efficiencies 1-6 for the interior radiation into the cylindrical cavity

plate according to equation (24) are shown in figure 8 unwrapped over the circumference. These, as well, are composed of the cavity modes, orthogonal over the structural interface.

5. Conclusion

This paper studies the orthogonal radiation properties of structural vibration with regard to an enclosed sound field. Using an analytical model, a general formulation for the acoustic potential energy is described in dependence of the

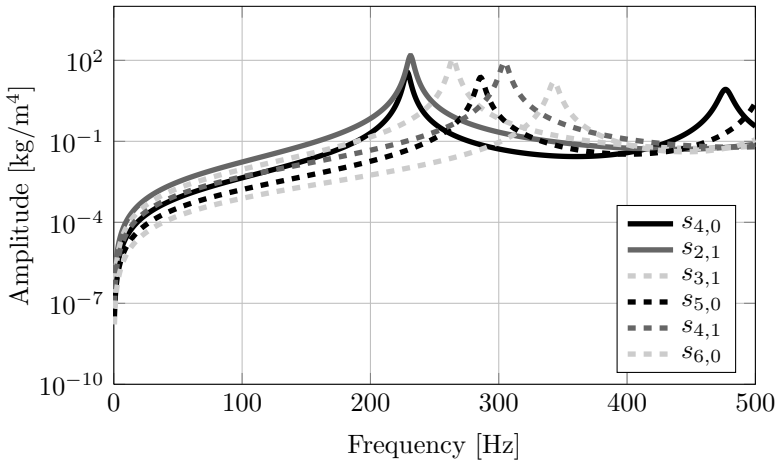

Figure 7: Radiation efficiencies 7-12 for the interior radiation into the cylindrical cavity

surrounding structural velocities. This formulation does not contain any structural modal information. The structural vibration is rather a boundary condition to the interior sound field. The resulting radiation modes of two generic systems of fluid-structure-interaction are then proven to be independent of frequency and they can be derived from the cavity modes on the interaction plane. The efficiencies of the interior sound radiation are a sum of the contributions from each parallel cavity mode at the interaction plane.
The frequency independence of the radiation modes offers a new perspective for fields like active control theory. In order to achieve a reduction of the acoustic potential energy in the cavity by active means, the controller must include only the frequency-independent radiation modes. The change of radiation modes with frequency can therefore be disregarded, which drastically reduces the computation costs for real-time applications. Future work will be focused on the global active control of cavity noise with structural radiation mode sensing.

Acknowledgement

This study has been conducted within the project *Transferzentrum - MRO und Cabin Upgrade* (project nr. LAHH 144), which is funded by the authority for Economy, Transport and Innovation of *Freie und Hansestadt Hamburg*.

References

[1] A. Baz, S. Poh, Performance of an active control system with piezoelectric actuators, Journal of sound and Vibration 126 (2) (1988) 327–343.

[2] C. R. Fuller, C. H. Hansen, S. D. Snyder, Active control of sound radiation from a vibrating rectangular panel by sound sources and vibration inputs:

an experimental comparison, Journal of Sound and Vibration 145 (2) (1991) 195–215.

[3] S. J. Elliott, M. E. Johnson, Radiation modes and the active control of sound power, The Journal of the Acoustical Society of America 94 (1993) 2194–2204.

[4] G. P. Gibbs, R. L. Clark, D. E. Cox, J. S. Vipperman, Radiation modal expansion: Application to active structural acoustic control, The Journal of the Acoustical Society of America 107 (1) (2000) 332–339.

[5] J. S. Bevan, T. L. Turner, Piezoceramic actuator placement for acoustic control of panels, Tech. Rep. NASA/CR-2001-211265, Old Dominion University, Norfolk, Virginia (2001).

[6] P. A. Nelson, S. J. Elliott, Active control of sound, Academic press, 1991.

[7] S. D. Snyder, N. Tanaka, On feedforward active control of sound and vibration using vibration error signals, The Journal of the Acoustical Society of America 94 (1993) 2181–2193.

[8] B. S. Cazzolato, C. H. Hansen, Active control of sound transmission using structural error sensing, The Journal of the Acoustical Society of America 104 (1998) 2878–2889.

[9] W. M. Johnson, Structural acoustic optimization of a composite cylindrical shell, Ph.D. thesis, G. W. Woodruff School of Mechanical Engineering (2004).

[10] W. M. Johnson, K. A. Cunefare, Use of principle velocity patterns in the analysis of structural acoustic optimization, The Journal of the Acoustical Society of America 121 (2) (2007) 938–948.

[11] F. J. Fahy, P. Gardonio, Sound and structural vibration: radiation, transmission and response, Academic press, 2007.

[12] B. S. Cazzolato, C. H. Hansen, Structural radiation mode sensing for active control of sound radiation into enclosed spaces, The Journal of the Acoustical Society of America 106 (1999) 3732–3735.

[13] A. K. Bagha, S. V. Modak, Structural sensing of interior sound for active control of noise in structural-acoustic cavities, The Journal of the Acoustical Society of America 138 (1) (2015) 11–21.

[14] S. Snyder, C. Hansen, The design of systems to control actively periodic sound transmission into enclosed spaces, part ii: mechanisms and trends, Journal of sound and vibration 170 (4) (1994) 451–472.

[15] J. Pan, C. Hansen, D. Bies, Active control of noise transmission through a panel into a cavity: I. analytical study, The Journal of the Acoustical Society of America 87 (5) (1990) 2098–2108.

[16] L. D. Pope, On the transmission of sound through finite closed shells: statistical energy analysis, modal coupling, and nonresonant transmission, The Journal of the Acoustical Society of America 50 (3B) (1971) 1004–1018.

[17] V. Jayachandran, S. M. Hirsch, J. Q. Sun, On the numerical modelling of interior sound fields by the modal function expansion approach, Journal of sound and vibration 210 (2) (1998) 243–254.

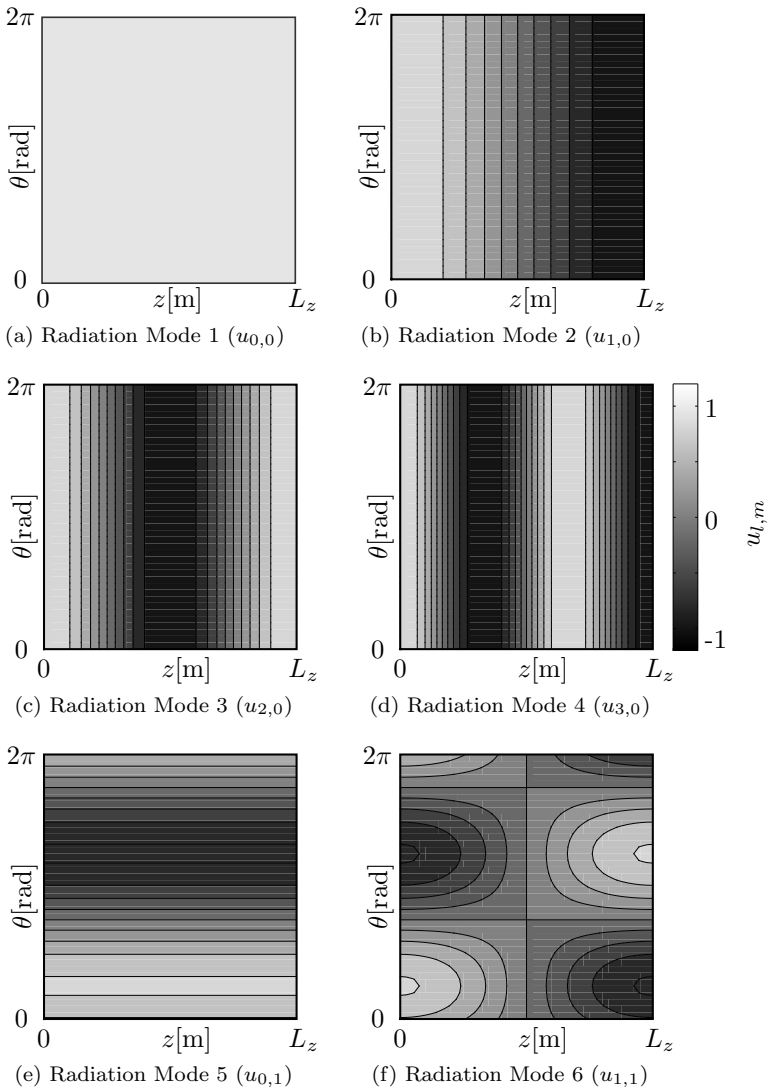

(a) Radiation Mode 1 ($u_{0,0}$)
(b) Radiation Mode 2 ($u_{1,0}$)
(c) Radiation Mode 3 ($u_{2,0}$)
(d) Radiation Mode 4 ($u_{3,0}$)
(e) Radiation Mode 5 ($u_{0,1}$)
(f) Radiation Mode 6 ($u_{1,1}$)

Figure 8: Radiation modes for the interior radiation into the cylindrical cavity